Application of hyperspectral and multispectral datasets for mineral mapping

D Rakhimov[1], *M* Juliev[2,3*], *I* Agzamova[4], *N* Normatova[4], *Ya* Ermatova[4], *D* Begimkulov[4], *L* Gafurova[5], M Hakimova[6] and *O* Ergasheva[5]

[1]Information-Analytical and Resources Center, Labzak street 1A, 100128 Tashkent, Uzbekistan
[2]Tashkent Institute of Irrigation and Agricultural Mechanization Engineers, Tashkent, 100000, Uzbekistan
[3]Turin Polytechnic University in Tashkent, Little Ring Road street 17, 100095 Tashkent, Uzbekistan
[4]Tashkent State Technical University, University street 2, 100095 Tashkent, Uzbekistan
[5]National University of Uzbekistan, University street 4, 100174 Tashkent, Uzbekistan
[6]Karshi engineering economics institute, Mustakillik street 225, 180100 Karshi, Uzbekistan

Abstract. In this study, hyperspectral datasets are simulated from multispectral data using a spectral reconstruction approach which is a sensor-independent technique. This technique makes use of information from atmospherically corrected multispectral Remote Sensing (MRS) data and normalized ground spectra for the simulation of HRS data. In this study EO-1, the ALI dataset was used for the simulation of hyperspectral Remote Sensing (HRS) data to discover the Udaipur region's unique minerals. A total of 61 spectral bands with 10 nm bandwidth were simulated. The simulated HRS data were validated using visual interpretation, statistical and classification approaches. Simulated HRS data from EO-1 Advanced Land Imager (ALI) has shown a high correlation with EO-1 Hyperion data. Spectral Angle Mapper (SAM) classification was also performed on simulated hyperspectral data for mineral mapping. It was observed that simulated hyperspectral data have shown comparable results with Hyperion and are better than their corresponding multispectral datasets.

1 Introduction

Multispectral Remote Sensing (MRS) from historical overview can be used for mineral mapping purposes [1]. A new era started in remote sensing when Hyperspectral Remote Sensing sensors emerge as an admirable make used for the congregation of contiguous spectral bands among the slender bandwidth to ranges from visible to Short Wave Infrared (SWIR) of the Electromagnetic Spectrum (ES) [2]. The multispectral data is enabled to wide-ranging to investigations the global earth surface is a peculiarity with the intention of embarrassed to collected with coarser bandwidth resolution datasets. HRS delivers spectral data comprising many bands in a solitary congregation as well as it has been a large area of applications visa-viz. mineralogy, reconnaissance, horticulture, and target recognition [2].

* Corresponding author: mukhiddinjuliev@gmail.com

The hyperspectral data applications of wide ranges distant from the sensors also have a few limitations. The large data storage capacities are required for sensitive detectors, Fast computers which make the acquisition and processing unwieldy and excessive [3]. In the present scenario, only one space-borne hyperspectral sensor i.e. EO-1 Hyperion with a 30m spatial resolution [3,4] and narrow swath (7.5 km) are available because a set of multispectral sensors providing the data among the comparable spatial resolution datasets is about the globe over the past few decades. The multispectral datasets due to the availability of enormous; it is certainly to need processing and simulate the hyperspectral data it is utilize the multispectral data with a bigger swath and high spatial resolution for detailed mineral mapping studies [5–8]. The identification and discrimination of hyperspectral data is to simulate the restrained variation pure spectra of a variety of features it will be present over the earth surface. Very few attempts were made in the past few years in the geo mineralogy field for simulation hyperspectral data using multispectral data. The technique takes place some methods using by spectral unmixing also various algorithms.

The Spectral unmixing is a method used for [9] finding the proportion of land surface and geological feature present inside a mixed pixel. A pixel in any satellite image is considered to be to mixed pixel when it has more than one land surface and geological feature. The occurrence of pure pixel is rare in the satellite data with a spatial resolution of 30m and the probability of more heterogeneous features within a single pixel increases with decreasing spatial resolution. Various unmixing techniques have been evolved for feature identification and extracting their percentage contribution in the mixed pixels of satellite data. Detailed mineral mapping is possible to find rare geo mineral rocks using simulated HRS data from MRS data. The main objective is mineral mapping using simulated to hyperspectral data from the multispectral data [4,10]. To Simulation of hyperspectral data from EO-1 ALI data and validation of simulated hyperspectral data with EO-1 Hyperion data using visual interpretation, statistical and spectral separability analysis and classification approaches. Comparative analysis of mineral map generated using EO-1 ALI multispectral data, simulated hyperspectral data from EO-1 ALI data and EO-1 Hyperion data.

Materials and data used.

To achieve the objective in the present study the following satellite data products, ancillary data, software and field surveyed data have been used.

The Earth Observation EO-1 Hyperion sensor has been developed by NASA's new millennium program in November 2000 [4]. The Hyperspectral Imager (Hyperion) instrument provides high quality data calibrated to sustain the inference of Earth observing missions of hyperspectral technology. The Hyperion sensors used to push broom spectrometer to scan the earth features and every image has to capture the spectrum line 30m along-track by 7.5 km [4]. There are 242 unique spectral spectrums covering as 357 – 2576 nm. The Level 1 Radiometric product has a total of 242 bands but only 198 bands are calibrated and overlap among the SWIR and VNIR focal planes and 196 of the unique channels to calibrated the range of SWIR 77-224 and 8-57 VNIR [11]. For the explanation are not calibrate of all 242 spectrum channels is mostly due to the detector's low responsively (Table 1). The bands are doing calibrate as a set of zero in those channels [11].

Table 1. Specification of EO-1 Hyperion.

Sensor altitude	705 Kms	**No. of rows**	256
Spatial resolution	30 meters	**No. of columns**	3128
Radiometric Resolution	16 bits	**VNIR**	0.45-1.35 μm
Swath	7.5 Km	**SWIR**	1.40-2.48 μm

The Multispectral (MS) Advanced Land Imager (ALI) the instrument is the principal instrument in the first EO-1 (Earth Observation-1) satellite [1]. The panchromatic spectrometer and multispectral is highly integrated into wide-angle optics that employs to ALI instrument [4]. In operation of push broom fashion with a swath width of 37 km and the orbital plane of 705 km of the earth surface. It has nine MS bands plus a Panchromatic (Pan) band, three more than ETM+, but does not have the thermal band. The MS bands of spatial resolution are the same as that of ETM+ (30 m) but it is better in the Pan band (10 m versus 15 m) (Table 2).

Spectroradiometer (SVC HR 1024) features. The HR-1024 from the Spectra Vista Corp. (SVC) is their newest high-performance single-beam field spectroradiometer measuring over the visible to short-wave infrared wavelength range (350-2500nm). We are using the data pre-processing ENVI 5.0 and ArcGIS for creating maps.

Table 2. Specification of EO-1 ALI.

Band	Wavelength(µm)	Ground Sample Distance(m)
PAN	0.48 - 0.69	10
MS - 1'	0.433 - 0.453	30
MS - 1	0.45 - 0.515	30
MS - 2	0.525 - 0.605	30
MS - 3	0.63 - 0.69	30
MS - 4	0.775 - 0.805	30
MS - 4'	0.845 - 0.89	30
MS - 5'	1.2 - 1.3	30
MS - 5	1.55 - 1.75	30

2 Materials and methods

The methodological approach is followed to data modeling and simulation of HRS data from MRS data using various techniques of processing satellite imagery [1]. The research has been divided into four phases: Data pre-processing e.g., ground observation data, hyperspectral simulation data and producing the mineral mapping. A detailed description of the methods adopted for the present study is enlightened in the block diagram in Figure 1.

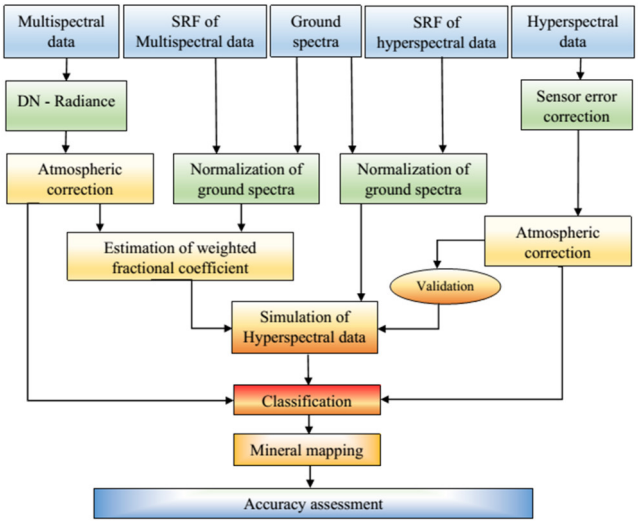

Fig. 1. Flowchart of the methodology.

3 Results and discussion

The Fast Line-of-sight Atmospheric Analysis of Hypercubes (FLAASH) atmospheric correction of EO-1 Hyperion data and EO-1 ALI model is used. Results before the discussion of spectral profiles anomaly and after the atmospheric correction of the datasets were compared by considering the atmospheric absorption and diagnostic absorption feature.

Weighted fractional coefficient images generated for each multispectral dataset after linear unmixing process. Each pixel in the fractional coefficient image is showing its abundance of each end member (vegetation, water, urban & agriculture). The abundance value ranges from zero to one. The pixels appearing brightest in the image corresponds to 1 i.e., showing maximum abundance whereas the pixel appearing darkest correspond to ground spectra which is submissive or doesn't contribute any abundance in the pixel.

From the EO-1 ALI, simulated data have been overall 61 spectral bands in the common wavelength range as of EO-1 Hyperion data [10]. The simulated HRS data is compared with EO-1 Hyperion data and it is observed that most of the bands appear same while preserving tone, texture, and shape. It observed that the spectra of randomly selected land features are retaining the diagnostic absorption characteristics.

Correlation between EO-1 Hyperion and simulated HRS data from EO-1 ALI data is calculated for validation of results. The spectral bands simulated to demonstrate a very high correlation indicating was observed for good simulation of the hyperspectral bands. The values of correlation coefficients for each simulated band from EO-1 ALI and EO-1 Hyperion band is given in the Table 3.

Table 3. Correlation between EO-1 Hyperion and Simulated HRS from ALI.

Bands	Correlation	Bands	Correlation	Bands	Correlation
1	0.71	**22**	0.85	**43**	0.81
2	0.82	**23**	0.85	**44**	0.81
3	0.90	**24**	0.86	**45**	0.82
4	0.91	**25**	0.86	**46**	0.82
5	0.91	**26**	0.87	**47**	0.82
6	0.90	**27**	0.87	**48**	0.82
7	0.90	**28**	0.86	**49**	0.82
8	0.90	**29**	0.85	**50**	0.81
9	0.89	**30**	0.82	**51**	0.81
10	0.89	**31**	0.82	**52**	0.82
11	0.89	**32**	0.82	**53**	0.82
12	0.90	**33**	0.81	**54**	0.82
13	0.90	**34**	0.81	**55**	0.81
14	0.91	**35**	0.81	**56**	0.81
15	0.87	**36**	0.78	**57**	0.81
16	0.87	**37**	0.78	**58**	0.81
17	0.87	**38**	0.80	**59**	0.81
18	0.83	**39**	0.81	**60**	0.61
19	0.81	**40**	0.81	**61**	0.61
20	0.79	**41**	0.81		
21	0.85	**42**	0.81		

In the study, spectral analysis has been carried out and to find out the comparison between image spectra of hyperspectral data (EO-1 Hyperion and simulated HRS data from MRS data) and field spectra of various mineral features. Equal weightage of 0.33 was given while performing spectral separability analysis using SAM.

Spectral Angle Mapper method has been used for classifying all the multispectral and their corresponding simulated hyperspectral datasets beside with Hyperion data for cross-validation. The classification results are shown from figures 2-5 the classifier outputs were further subjected to accuracy assessment and the results are shown in Tables 4-6.

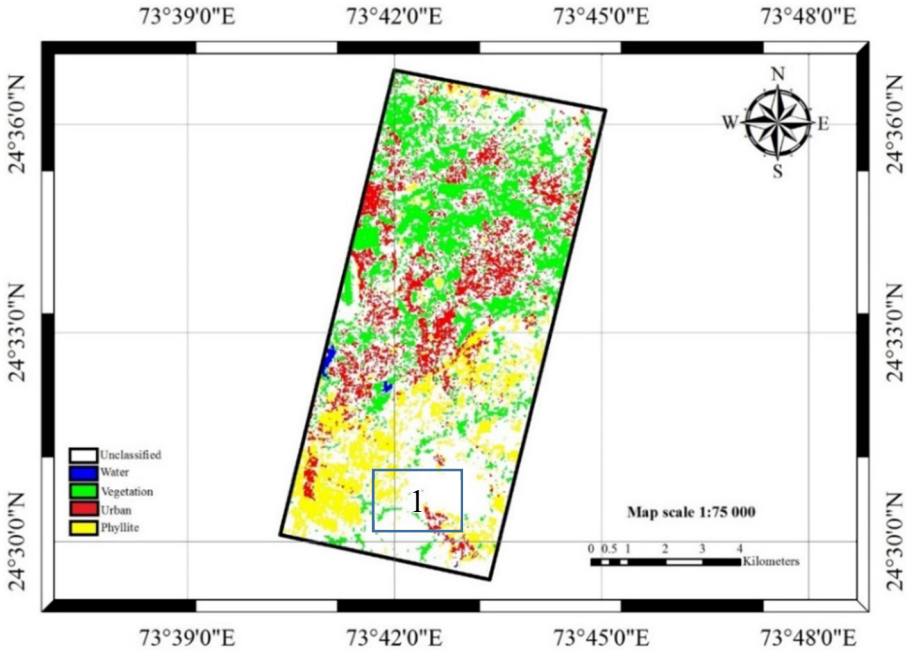

Fig. 2. Classified EO-1 Hyperion data.

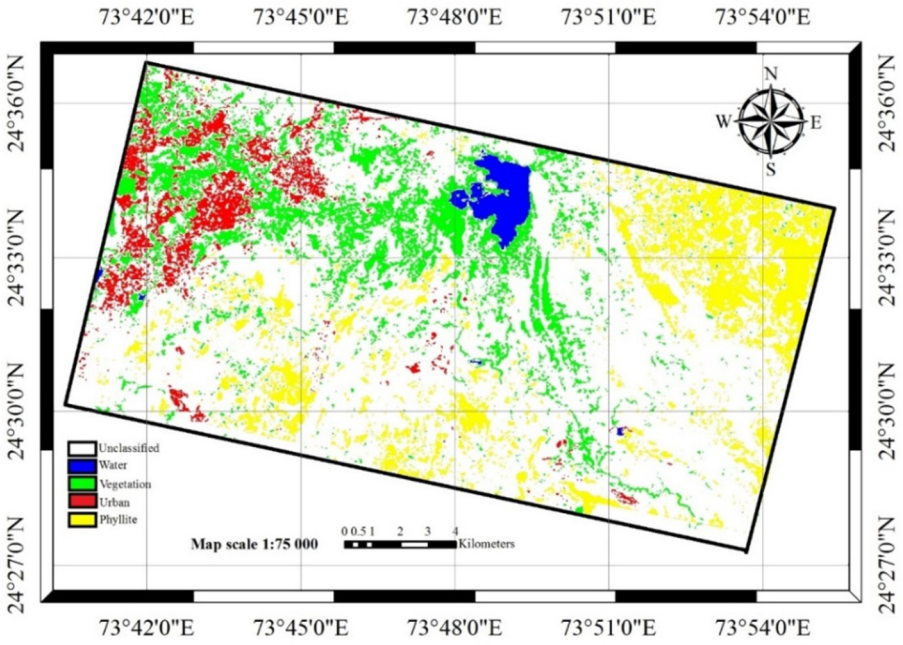

Fig. 3. Classified EO-1 ALI data.

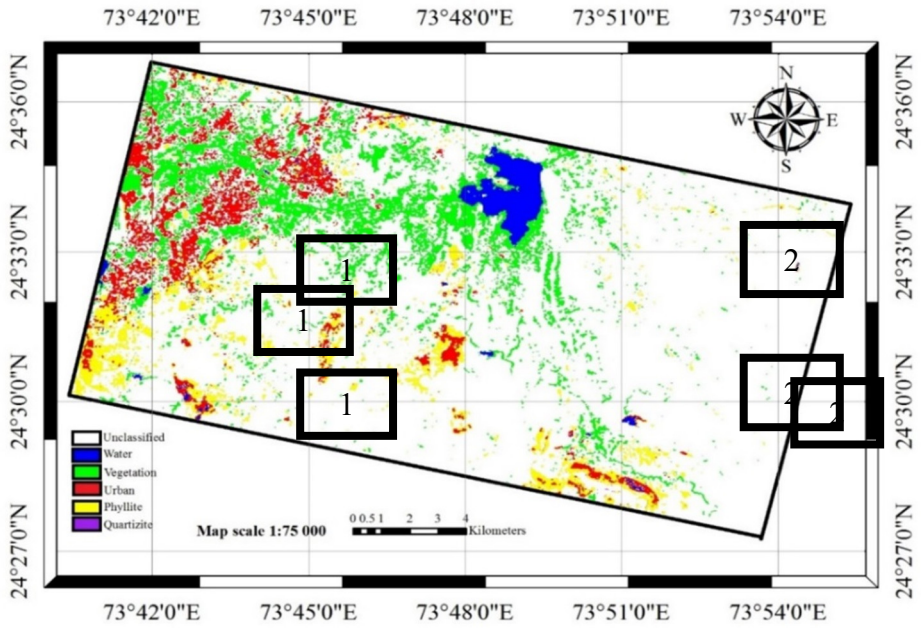

Fig. 4. Classified simulated HRS data (from EO-1 ALI).

Table 4. Accuracy assessment of all classified results.

Spatial resolution	Classified Map	Overall Accuracy	Kappa Coefficient
30 m	EO-1 Hyperion	72.402	0.6320
30 m	Simulated HRS (from EO-1ALI) data	81.63	0.725
30 m	EO-1 ALI	67.11	0.602

Table 5. Accuracy Assessment of EO-1 Hyperion.

Class	Producer's Accuracy	User's Accuracy
Vegetation	94.74	80.00
Water	68.97	100
Urban	63.64	66.67
Phyllite	70.45	100.00

Table 6. Accuracy Assessment EO-1 ALI& simulated HRS (from EO-1ALI) data.

	EO-1 ALI data		simulated HRS (from EO-1ALI) data	
Class	**Producer's Accuracy**	**User's Accuracy**	**Producer's Accuracy**	**User's Accuracy**
Vegetation	84.44	97.44	91.43	99.56
Water	100	100	100	100
Urban	67.57	100	76.36	75.00
Phyllite	34.78	100	73.08	67.86
Quartzite	0	0	51.47	81.40

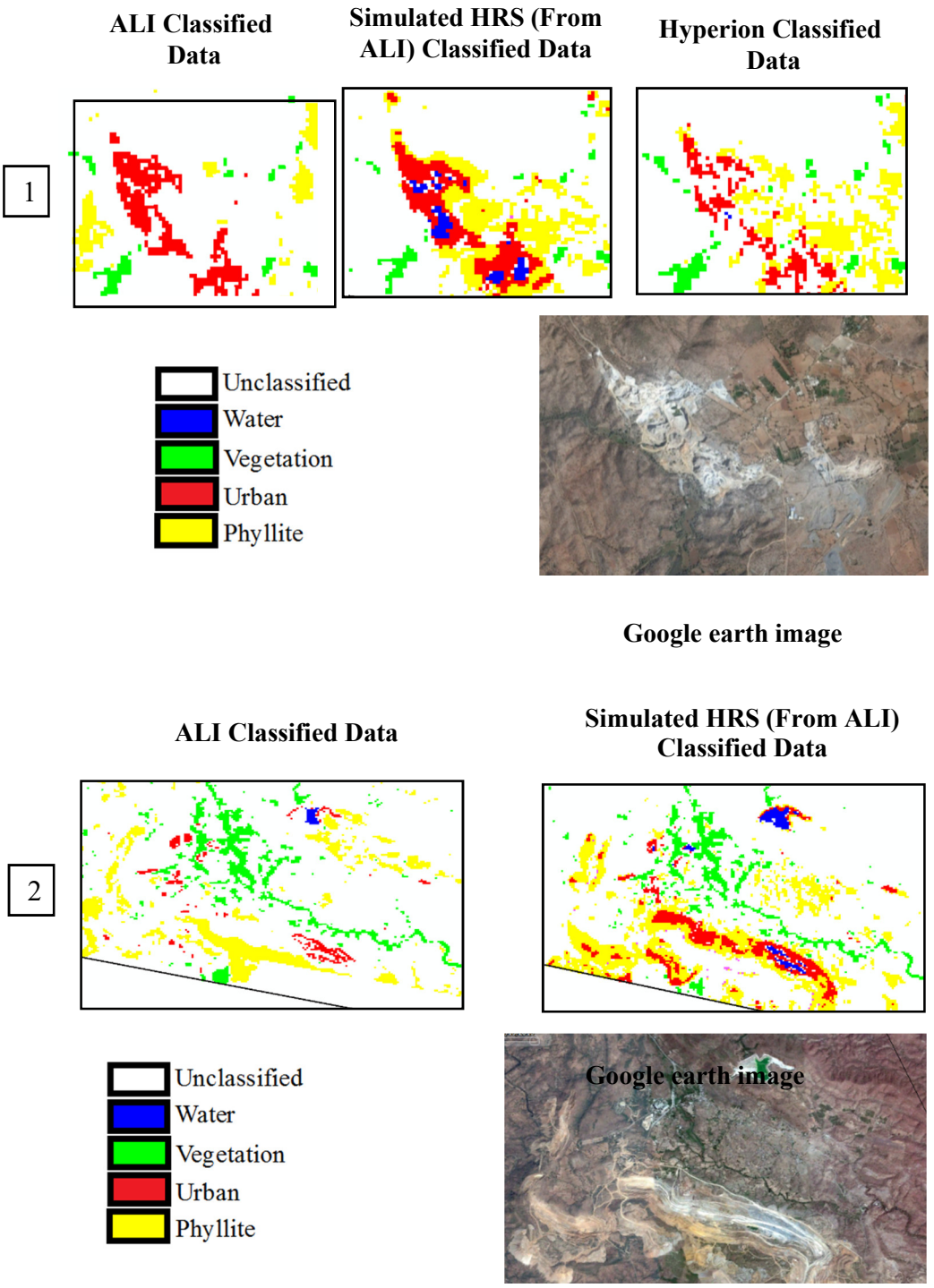

Fig. 5. Comparative analysis of all the classified data and google earth image.

Following observations are made from the classification and accuracy assessment results:

- Overall accuracy and kappa coefficient of all the classified products obtained from simulated HRS data is improved as compared to their corresponding classified products derived from multispectral data.
- The extent of misclassification which was observed in the classified MRS products are reduced significantly in the classified products of simulated HRS data.
- Majority of mineral class phyllite has shown improved classification results in the classified products generated from simulated data.
- The classified result is obtained from the pure spectra analysis to simulated products are able to discriminate minerals and land use land cover (LULC) classes of similar nature e.g., urban which are limitation of products generated from multispectral dataset.

4 Conclusions

The research work has been carried out to discuss the summary of the objectives accomplished with the scope of future advancement. It involves to the simulation of HRS data from available multispectral to create the mineral map. Simulated HRS from MRS data also it shows how it is effectively influencing mineral mapping application. Finally, the simulation HRS data from EO-1 ALI has shown high correlation with EO-1 Hyperion data. Spectral Angle Mapper (SAM) classification was also performed on simulated hyperspectral data for mineral mapping. It was observed that simulated hyperspectral data have shown comparable results with Hyperion and better than their corresponding multispectral datasets.

References

1. V. Tiwari, V. Kumar, K. Pandey, R. Ranade, S. Agarwal, *Simulation of the hyperspectral data from multispectral data using Python programming language*, J. SPIE Asia-Pacific Remote Sensing, ed A M Larar, P Chauhan, M Suzuki and J Wang, 98800W (New Delhi, India, 2016)
2. K. Muramatsu, S. Furumi, N. Fujiwara, A. Hayashi, M. Daigo, F. Ochiai, *Pattern decomposition method in the albedo space for Landsat TM and MSS data analysis,* International Journal of Remote Sensing**, 21,** 99-119 (2000)
3. J. M. Bioucas-Dias, A. Plaza, N. Dobigeon, M. Parente, Q. Du, P. Gader, J. Chanussot, *Hyperspectral Unmixing Overview: Geometrical, Statistical and Sparse Regression-Based Approaches,* IEEE J. Sel. Top. Appl. Earth Observations Remote Sensing, **5,** 354-79 (2012)
4. R. Cavalli, L. Fusilli, S. Pascucci, S. Pignatti, F. Santini, *Hyperspectral Sensor Data Capability for Retrieving Complex Urban Land Cover in Comparison with Multispectral Data: Venice City Case Study,* J. Sensors, **8,** 3299-320 (Italy, 2008)
5. I. Mondal, S. Thakur, M. Juliev, J. Bandyopadhyay, T. K. De, *Spatio-temporal modelling of shoreline migration in Sagar Island*, J Coast Conserv, **24,** 50 (West Bengal, India, 2020)
6. I. Mondal, S. Thakur, M. Juliev, De. T. Kumar, *Comparative analysis of forest canopy mapping methods for the Sundarban biosphere reserve*, J. Environ Dev Sustain, **23** 15157-82 (West Bengal, India 2021)
7. M. Juliev, A. Pulatov, S. Fuchs, J. Hübl, *Analysis of Land Use Land Cover Change*

Detection of Bostanlik District, Uzbekistan, Polish Journal of Environmental Studies, **28,** 3235-42 (2019)

8. M. Juliev, A. Pulatov, J. Hubl, *Natural hazards in mountain regions of Uzbekistan: A review of mass movement processes in Tashkent province,* International Journal of Scientific & Engineering Research, **8,** 1102-8 (2017)
9. D. C. Heinz, Chein-I-Chang, F*ully constrained least squares linear spectral mixture analysis method for material quantification in hyperspectral imagery,* IEEE Trans. Geosci. Remote Sensing, **39,** 529-45 (2001)
10. B. Liu, L. Zhang, X. Zhang, B. Zhang, Q. Tong, *Simulation of EO-1 Hyperion Data from ALI Multispectral Data Based on the Spectral Reconstruction Approach, J*. Sensors**, 9,** 3090-108 (2009)
11. A. Miglani, S. S. Ray, R. Pandey, J. S. Parihar, *Evaluation of EO-1 hyperion data for agricultural applications,* J Indian Soc Remote Sens, **36** 255-66 (2008)